

On the dispersion of waves propagating in “plate+fluid layer” systems

Surkay D. Akbarov^{1,2} and Masoud Negin^{*3}

¹Department of Mechanical Engineering, Yildiz Technical University, Istanbul, Turkey

²Institute of Mathematics and Mechanics of the Azerbaijan National Academy of Sciences, Baku, Azerbaijan

³Department of Civil Engineering, Bahcesehir University, Istanbul, Turkey

(Received January 24, 2021, Revised May 14, 2021, Accepted May 15, 2021)

Abstract. The paper deals with the study of the dispersion of quasi-Lamb waves in a hydro-elastic system consisting of an elastic plate, barotropic compressible inviscid fluid, and rigid wall. The motion of the plate is described using the exact equations of elastodynamics, however, the flow of the fluid using the linearized equations and relations of the Navier-Stokes equations. The corresponding dispersion equation is obtained and this equation is solved numerically, as a result of which the corresponding dispersion curves are constructed. The main attention is focused on the effect of the presence of the fluid and the effect of the fluid layer thickness (i.e., the fluid depth) on the dispersion curves. The influence of the problem parameters on the dispersion curves related to the quasi-Scholte wave is also considered. As a result of the analyses of the numerical results, concrete conclusions are made about the influence of the fluid depth, the rigid wall restriction on the fluid motion, and the material properties of the constituents on the dispersion curves. During the analyses, the zeroth and the first four modes of the propagating waves are considered.

Keywords: quasi-lamb waves; wave dispersion; quasi-Scholte waves; elastic layer; hydro-elastic system; compressible inviscid fluid

1. Introduction

One of the main questions of the dynamics of plate-fluid hydro-elastic systems concerns the dispersion of propagating waves in these systems. The results of investigations on the problem provide the theoretical basis for non-destructive defect determination in hydro-elastic systems with ultrasonic waves. The investigations carried out in the present paper are about finding the answer to this question. In this way, we studied the dispersion of the quasi-Lamb waves propagating in the hydro-elastic system consisting of an elastic plate, compressible inviscid fluid layer, and rigid wall restricting the motion of the fluid in the direction perpendicular to the plate plane. To illustrate the novelty of the investigations carried out in the present paper we first consider a brief review of the related and relatively recent investigations. Note that the review of earlier investigations can be found in the works of Viktorov (1967), Bagno (1997) and Akbarov (2018).

We begin this review with the paper by Bagno (2015) in which the wave dispersion in the hydro-elastic system consisting of the pre-stressed compressible elastic plate and compressible inviscid

*Corresponding author, Ph.D., E-mail: masoud.negin@eng.bau.edu.tr

fluid layer with a free face surface is studied. Following the investigations carried out in this paper Bagno (2016) developed his work for the case where the fluid is viscous and later, in the paper (Bagno 2017) he considered the case where the elastic plate is in contact with the inviscid compressible fluid half-space. In all these investigations the flow of the fluid is described by utilizing the linearized Navier-Stokes equations and the motion of the plate by utilizing the three-dimensional linearized theory of elastic waves in bodies with initial stresses. In the paper (Guz and Bagno 2016) the investigation carried out in the paper (Bagno 2016) again is considered for the case where the plate has initial stresses and corresponding numerical results are presented for large change range of the problem parameters. Guz and Bagno (2019) then considered the problem related to the wave dispersion in the elastic plate which is in contact with the compressible viscous fluid.

Thus, it follows from the foregoing brief review that almost all investigations regarding the plate and fluid interaction problem relate to the cases where the plate is in contact with the fluid half-space or is in the contact with a fluid layer with the free surface. However, there are many situations where the walls restrict the flow of the fluid that is in contact with the plate. In such cases, the corresponding hydro-elastic systems are modeled as “plate+fluid+rigid wall” system. There are a considerable number of investigations such as Akbarov and Ismailov (2015, 2016, 2017, 2018), Akbarov and Panakhli (2017), Akbarov and Huseynova (2019, 2020) related to the dynamics, the forced vibration and moving load regarding this system. We briefly discuss the subjects of these papers. The paper (Akbarov and Ismailov 2015) studies the dynamics of the moving load acting on the “plate+fluid+rigid wall” system. The numerical results related to the interface stress and fluid flow velocities are presented and discussed. The forced vibration of the “plate + fluid + rigid wall” system is investigated in the paper (Akbarov and Ismailov 2017) and the rule of the influence of the fluid viscosity and compressibility on the interface stress and fluid flow velocities are established. The paper (Akbarov and Ismailov 2016) investigates the dynamics of the oscillating moving load acting on the mentioned system. As a result of this investigation, the “gyroscopic effect” on plate fluid interaction characteristics is established. The forced vibration of the “viscoelastic plate + viscous fluid + rigid wall” system is studied in the paper (Akbarov and Ismailov 2018). Numerical results on the influence of the rheological parameters of the plate material on the interface stress and fluid flow velocities are presented and discussed. The paper (Akbarov and Panakhli 2017) studies the forced vibration of the hydro-elastic system consisting of the moving plate, compressible viscous fluid and rigid wall. Numerical results regarding the influence of the plate moving velocity on the stress and velocity state in the hydro-elastic system under consideration are presented and discussed. Note that in all the foregoing papers it is assumed that the plate material is isotropic. The paper (Akbarov and Huseynova 2019) unlike the foregoing works investigates forced vibration of the hydro-elastic system consisting of the orthotropic plate, compressible viscous fluid and rigid wall. Numerical results illustrated the influence of the anisotropy properties of the plate material on the stress and velocity field in the system are analyzed. Finally, the paper (Akbarov and Huseynova 2020) studies the fluid flow profile in the system “orthotropic plate+compressible viscous fluid + rigid wall” under action on the plate the moving load.

Thus, it follows from the foregoing review and from the authors’ best knowledge, up to now, there are not any investigations related to the guided wave dispersion propagating in the “plate+compressible fluid+rigid wall”. Considering that the significance of such investigation is not limited only to the theoretical senses, in the present paper we attempt to investigate the dispersion of the waves propagating in the system consisting of an elastic plate, compressible inviscid fluid, and rigid wall.

2. Field equations and basic relations

We consider wave propagation in a hydro-elastic system consisting of an elastic layer, compressible barotropic inviscid fluid layer and rigid wall the sketch of which is illustrated in Fig. 1(a). Associate the Cartesian system of coordinates $Ox_1x_2x_3$ with the upper face plane of the plate and as we will consider the plane-stain state in the elastic plate and the plane flow of the fluid layer in the Ox_1x_2 plane, therefore the Ox_3 axis doesn't shown in Fig. 1(a). According to the selected coordinate system and to Fig. 1(a), we can indicate the regions $\{-\infty < x_1 < +\infty, -h \leq x_2 \leq 0, -\infty < x_3 < +\infty\}$ and $\{-\infty < x_1 < +\infty, -h_d \leq x_2 \leq -h, -\infty < x_3 < +\infty\}$ occupied by the elastic plate and fluid layer, respectively, where h is the plate thickness and h_d is the fluid depth or the thickness of the fluid layer.

Thus, within the scope of the foregoing assumptions, we can write the following equations and relations describing the motion for the elastic plate

Equations of motion

$$\frac{\partial \sigma_{11}}{\partial x_1} + \frac{\partial \sigma_{12}}{\partial x_2} = \rho \frac{\partial^2 u_1}{\partial t^2}, \quad \frac{\partial \sigma_{12}}{\partial x_1} + \frac{\partial \sigma_{22}}{\partial x_2} = \rho \frac{\partial^2 u_2}{\partial t^2}, \quad (1)$$

Elasticity relations

$$\sigma_{11} = (\lambda + 2\mu)\varepsilon_{11} + \lambda\varepsilon_{22}, \quad \sigma_{22} = \lambda\varepsilon_{11} + (\lambda + 2\mu)\varepsilon_{22}, \quad \sigma_{12} = 2\mu\varepsilon_{12}, \quad (2)$$

Strain-displacement relations

$$\varepsilon_{11} = \frac{\partial u_1}{\partial x_1}, \quad \varepsilon_{22} = \frac{\partial u_2}{\partial x_2}, \quad \varepsilon_{12} = \frac{1}{2} \left(\frac{\partial u_1}{\partial x_2} + \frac{\partial u_2}{\partial x_1} \right). \quad (3)$$

In Eqs. (1)-(3) σ_{11} , σ_{22} and σ_{12} (ε_{11} , ε_{22} and ε_{12}) are the components of the stress (strain) tensor, u_1 and u_2 are the components of the displacement vector, λ and μ are the Lamé's constants and ρ is the density of the material of the elastic layer.

Now we write the field equations for fluid flow.

Linearized equations of the fluid flow:

Linearized Navier-Stokes, continuity, rheological, strain-velocity dependencies and state equations for compressible inviscid fluid layer can be respectively written as follows

$$\rho_0^{(1)} \frac{\partial v_1}{\partial t} + \frac{\partial p^{(1)}}{\partial x_1} = 0, \quad \rho_0^{(1)} \frac{\partial v_2}{\partial t} + \frac{\partial p^{(1)}}{\partial x_2} = 0, \quad (4)$$

Linearized continuity equation

$$\frac{\partial \rho^{(1)}}{\partial t} + \rho_0^{(1)} \left(\frac{\partial v_1}{\partial x_1} + \frac{\partial v_2}{\partial x_2} \right) = 0, \quad (5)$$

The components of the stress tensor in the fluid are determined through the relations

$$T_{ij} = -\delta_{ij} p^{(1)}, \quad (6)$$

Linearized state equation

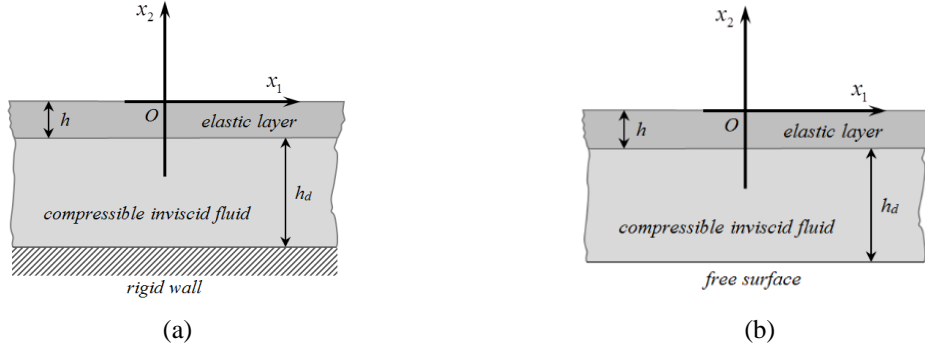


Fig. 1 Geometry of the problem

$$\frac{\partial p^{(1)}}{\partial \rho^{(1)}} = a_0^2. \quad (7)$$

In (4)-(7) the following notation is used: $\rho_0^{(1)}$ is the fluid density before perturbation, $\rho^{(1)}$ and $p^{(1)}$ are perturbations of the fluid density and pressure, respectively, a_0 is a sound speed in the fluid, v_1 and v_2 are components of the fluid flow velocity vector, T_{11} and T_{22} are components of the stress tensor in the fluid.

Note that the explanation of how the linearized equations in (4) and (5) are obtained, is given in the Appendix.

According to Guz (2009), the solution of the above system of Eqs. (4)-(7) is reduced to finding the potential φ determined from the following equation

$$\left(\Delta - \frac{1}{a_0^2} \frac{\partial^2}{\partial t^2} \right) \varphi = 0. \quad (8)$$

Note that the components of the velocity vector v_1 , v_2 and the pressure $p^{(1)}$ are expressed by the this potential through the following expressions

$$v_1 = \frac{\partial \varphi}{\partial x_1}, \quad v_2 = \frac{\partial \varphi}{\partial x_2}, \quad p^{(1)} = -\rho_0^{(1)} \frac{\partial \varphi}{\partial t}, \quad \rho^{(1)} = -\frac{\rho_0^{(1)}}{a_0^2} \frac{\partial \varphi}{\partial t}. \quad (9)$$

Substituting the presentation in (9) into the equations in (4) it is obtained that these equations are satisfied automatically. Moreover, substituting the presentation in (9) into the continuity equation in (5) it is obtained Eq. (8) with respect to the potential φ . If we assume that the fluid is incompressible, then we must obtain limit case of Eqs. (8) and (9) as $a_0 \rightarrow \infty$, as a result of which it is attained the equation $\Delta \varphi = 0$ instead of Eq. (8) and $\rho^{(1)} = 0$ instead of the last presentation in (9). Consequently, the presentation $\vec{v} = \overline{\text{grad}} \varphi$ useable not only for the incompressible fluids but also for the barotropic compressible fluids.

This completes the field equations and we assume that for the problem under consideration the following boundary, compatibility and impermeability conditions are satisfied.

Boundary conditions on the upper free plane of the plate

$$\sigma_{12}|_{x_2=0} = 0, \quad \sigma_{22}|_{x_2=0} = 0. \quad (10)$$

Compatibility conditions on the contact plane between the fluid and plate

$$\sigma_{12}|_{x_2=-h} = 0, \quad \sigma_{22}|_{x_2=-h} = T_{22}|_{x_2=-h}, \quad \frac{\partial u_2}{\partial t} \Big|_{x_2=-h} = v_2|_{x_2=-h}. \quad (11)$$

Impermeability condition on the rigid wall

$$v_2|_{x_2=-h-h_d} = 0. \quad (12)$$

This completes the formulation of the problem which we are going to investigate in the present paper. Nevertheless, we note that, as usual, the wave propagation problem for the “elastic plate+fluid layer system” were investigated for the case where the layer face, as in the paper by Bagno (2015) is free from the restriction on the flow velocity, such as shown in Fig. 1(b) and in this case the condition

$$T_{22}|_{x_2=-h-h_d} = -P'|_{x_2=-h-h_d} = 0 \quad (13)$$

is written instead of the condition (12).

The question “how the aforementioned restriction can act on the wave dispersion in the hydro-elastic system under consideration?” will be also considered in the present investigation.

It follows from the above formulation that the elastic and fluid flow fields are coupled only through the compatibility conditions (11). In other words, the governing field equations of each constituent do not contain the quantity related to the other constituent. However, there are many other problems related to the coupling of the electric, magnetic, thermal, and mechanical fields simultaneously, such as the problems considered in the papers by Mororro-Navarro *et al.* (2017, 2018, 2020) and many others listed therein, in which the equations of the mechanical and thermal fields contain the terms determined by the electromechanical fields and vice-versa. Consequently, in the mentioned type problems, the coupling of the various fields is accomplished through the field equations, which complicates the solution of the corresponding mathematic problem, where numerical methods are required, as for instance, the numerical methods developed in the papers Mororro-Navarro *et al.* (2017, 2018, 2020).

3. Method of solution

As we consider the harmonic waves propagating in the Ox_1 axis direction, therefore the components of the displacement vector for elastic layer can be presented as $u_j = \bar{u}_j(x_2)e^{i(kx_1 - \omega t)}$ and substituting this presentations into Eqs. (3) and (2) we obtain the following equations for the amplitudes $\bar{u}_j(x_2)$ ($j=1,2$) from Eq. (1)

$$\begin{cases} \frac{d^2 \bar{u}_1}{d(kx_2)^2} + c_{11} \frac{d\bar{u}_1}{d(kx_2)} + c_{12} \bar{u}_1 = 0, \\ \frac{d^2 \bar{u}_2}{d(kx_2)^2} + c_{21} \frac{d\bar{u}_2}{d(kx_2)} + c_{22} \bar{u}_2 = 0, \end{cases} \quad (14)$$

where

$$\begin{aligned} c_{11} &= \frac{\lambda + \mu}{\mu} i, & c_{12} &= \frac{c^2}{c_2^2} - \frac{\lambda + 2\mu}{\mu}, & c_2 &= \sqrt{\mu/\rho}, \\ c_{21} &= \frac{\lambda + \mu}{\lambda + 2\mu} i, & c_{22} &= \frac{c^2}{c_1^2} - \frac{\mu}{\lambda + 2\mu}, & c_1 &= \sqrt{(\lambda + 2\mu)/\rho}. \end{aligned} \quad (15)$$

After some mathematical manipulations we derive the following equation for $\bar{u}_2(x_2)$ from Eq. (14)

$$\frac{d^4 \bar{u}_2}{d(kx_2)^4} + C_1 \frac{d^2 \bar{u}_2}{d(kx_2)^2} + C_2 \bar{u}_2 = 0. \quad (16)$$

The general solution of Eq. (16) is determined as follows

$$\bar{u}_2(x_2) = A_1 \exp(R_1 kx_2) + A_2 \exp(-R_1 kx_2) + A_3 \exp(R_2 kx_2) + A_4 \exp(-R_2 kx_2), \quad (17)$$

where

$$\begin{cases} R_1 = \sqrt{-\frac{C_1}{2} + \sqrt{\frac{C_1^2}{4} - C_2}}, & R_2 = \sqrt{-\frac{C_1}{2} - \sqrt{\frac{C_1^2}{4} - C_2}}, \\ C_1 = c_{22} + c_{12} - c_{11}c_{21}, & C_2 = c_{12}c_{22} \end{cases} \quad (18)$$

Using the solution (17) we determine also the expression for the function $\bar{u}_1(x_2)$ from Eq. (14) as

$$\bar{u}_1(x_2) = A_1 a_1 \exp(R_1 kx_2) + A_2 a_2 \exp(-R_1 kx_2) + A_3 a_3 \exp(R_2 kx_2) + A_4 a_4 \exp(-R_2 kx_2), \quad (19)$$

where

$$a_1 = \frac{c_{22} - R_1^2}{c_{21}R_1}, \quad a_2 = -\frac{c_{22} - R_1^2}{c_{21}R_1}, \quad a_3 = \frac{c_{22} - R_2^2}{c_{21}R_2}, \quad a_4 = -\frac{c_{22} - R_2^2}{c_{21}R_2}. \quad (20)$$

Note that there are not any conditions on the C_1 and C_2 in order to prevent becoming the complex values of the R_1 and R_2 in (18). However, under concrete numerical investigations carried out in the present paper the values of the R_1 and R_2 are obtained always real values.

Substituting the expressions in (17) and (19) into the relation in (3) we determine the expression for the components of strain tensor and the substituting these later expressions into the elasticity relations in (2) we obtain the following expressions for the stresses which enter the boundary and compatibility conditions

$$\begin{aligned} \sigma_{12} &= \mu [A_1 k(a_1 R_1 + i) \exp(R_1 kx_2) + A_2 k(-a_2 R_1 + i) \exp(-R_1 kx_2) + \\ &\quad A_3 k(a_3 R_2 + i) \exp(R_2 kx_2) + A_4 k(-a_4 R_2 + i) \exp(-R_2 kx_2)], \\ \sigma_{22} &= A_1 k((\lambda + 2\mu)R_1 + i\lambda a_1) \exp(R_1 kx_2) + A_2 k(-(\lambda + 2\mu)R_1 + i\lambda a_2) \exp(-R_1 kx_2) + \\ &\quad A_3 k((\lambda + 2\mu)R_2 + i\lambda a_3) \exp(R_2 kx_2) + A_4 k(-(\lambda + 2\mu)R_2 + i\lambda a_4) \exp(-R_2 kx_2). \end{aligned} \quad (21)$$

This completes the determination of the values related to the elastic plate.

Now we consider the determination of the values related to the fluid and according to the

foregoing discussions we represent the potential φ as $\varphi = \bar{\varphi}(x_2)e^{i(kx_1 - \omega t)}$. Substituting this expression into Eq. (8) we obtain the following equation for the amplitude of this potential

$$\frac{d^2\bar{\varphi}}{d(kx_2)^2} - \left(1 - \frac{c^2}{a_0^2}\right)\bar{\varphi} = 0. \quad (22)$$

Thus, we obtain the following expression from Eq. (16) for the amplitude of the potential $\bar{\varphi}(x_2)$

$$\bar{\varphi}(x_2) = B_1 \exp(\delta k x_2) + B_2 \exp(-\delta k x_2), \quad (23)$$

where

$$\delta = \sqrt{1 - (c^2/a_0^2)}, \quad (24)$$

and $c(=\omega/k)$ is the phase velocity of the propagated waves.

Substituting the expression (23) into the relations in (9) we obtain the following expressions for the fluid pressure and velocity which enter into the compatibility (11) and impermeability (12) conditions.

$$\begin{aligned} p^{(1)} &= -\rho_0^{(1)} i \omega (B_1 \exp(\delta k x_2) + B_2 \exp(-\delta k x_2)), \\ V_2 &= B_1 k \delta \exp(\delta k x_2) - B_2 k \delta \exp(-\delta k x_2). \end{aligned} \quad (25)$$

Finally, substituting the expressions in (19), (21) and (25) into the boundary (10), compatibility (11) and impermeability (12) conditions, we obtain the system of homogeneous linear algebraic equations with respect to the unknowns A_1, A_2, A_3, A_4, B_1 and B_2 . This system of equations can be presented in a matrix form as follows

$$\mathbf{AX} = \mathbf{0}, \quad \mathbf{A} = \begin{pmatrix} \alpha_{11} & \alpha_{12} & \alpha_{13} & \alpha_{14} & \alpha_{15} & \alpha_{16} \\ \alpha_{21} & \alpha_{22} & \alpha_{23} & \alpha_{24} & \alpha_{25} & \alpha_{26} \\ \alpha_{31} & \alpha_{32} & \alpha_{33} & \alpha_{34} & \alpha_{35} & \alpha_{36} \\ \alpha_{41} & \alpha_{42} & \alpha_{43} & \alpha_{44} & \alpha_{45} & \alpha_{46} \\ \alpha_{51} & \alpha_{52} & \alpha_{53} & \alpha_{54} & \alpha_{55} & \alpha_{56} \\ \alpha_{61} & \alpha_{62} & \alpha_{63} & \alpha_{64} & \alpha_{65} & \alpha_{66} \end{pmatrix}, \quad \mathbf{X} = \begin{pmatrix} A_1 \\ A_2 \\ A_3 \\ A_4 \\ B_1 \\ B_2 \end{pmatrix}, \quad (26)$$

where

$$\begin{aligned} \alpha_{11} &= \mu k (a_1 R_1 + i), \quad \alpha_{12} = \mu k (-a_2 R_1 + i), \quad \alpha_{13} = \mu k (a_3 R_2 + i), \quad \alpha_{14} = \mu k (-a_4 R_2 + i), \quad \alpha_{15} = 0, \quad \alpha_{16} = 0, \\ \alpha_{21} &= k((\lambda + 2\mu)R_1 + i\lambda a_1), \quad \alpha_{22} = k(-(\lambda + 2\mu)R_1 + i\lambda a_2), \\ \alpha_{23} &= k((\lambda + 2\mu)R_2 + i\lambda a_3), \quad \alpha_{24} = k(-(\lambda + 2\mu)R_2 + i\lambda a_4), \quad \alpha_{25} = 0, \quad \alpha_{26} = 0, \\ \alpha_{31} &= \mu k (a_1 R_1 + i) \exp(-R_1 kh), \quad \alpha_{32} = \mu k (-a_2 R_1 + i) \exp(R_1 kh), \\ \alpha_{33} &= \mu k (a_3 R_2 + i) \exp(-R_2 kh), \quad \alpha_{34} = \mu k (-a_4 R_2 + i) \exp(R_2 kh), \quad \alpha_{35} = 0, \quad \alpha_{36} = 0, \\ \alpha_{41} &= k((\lambda + 2\mu)R_1 + i\lambda a_1) \exp(-R_1 kh), \quad \alpha_{42} = k(-(\lambda + 2\mu)R_1 + i\lambda a_2) \exp(R_1 kh), \\ \alpha_{43} &= k((\lambda + 2\mu)R_2 + i\lambda a_3) \exp(R_2 kh), \quad \alpha_{44} = k(-(\lambda + 2\mu)R_2 + i\lambda a_4) \exp(R_2 kh), \\ \alpha_{45} &= -\rho_0^{(1)} i \omega \exp(-\delta kh), \quad \alpha_{46} = -\rho_0^{(1)} i \omega \exp(\delta kh), \\ \alpha_{51} &= i \omega \exp(-R_1 kh), \quad \alpha_{52} = i \omega \exp(R_1 kh), \quad \alpha_{53} = i \omega \exp(-R_2 kh), \quad \alpha_{54} = i \omega \exp(R_2 kh), \end{aligned}$$

$$\begin{aligned}
\alpha_{55} &= -k\delta \exp(-\delta kh), \quad \alpha_{56} = k\delta \exp(\delta kh), \\
\alpha_{61} &= 0, \quad \alpha_{62} = 0, \quad \alpha_{63} = 0, \quad \alpha_{64} = 0, \\
\alpha_{65} &= k\delta \exp(-\delta k(h+h_d)), \quad \alpha_{66} = -k\delta \exp(\delta k(h+h_d)).
\end{aligned} \tag{27}$$

To obtain non-trivial solutions to system of the homogeneous linear system of Eq. (26), it is necessary that

$$\det \mathbf{A} = \det \|\alpha_{ij}\| = 0, \quad i, j = 1, 2, \dots, 6. \tag{28}$$

where the components α_{ij} of the matrix \mathbf{A} are determined through the expressions in (27).

This completes the consideration of the solution to the field equations and obtaining the corresponding dispersion equation for investigation of the dispersion of the wave propagated in the hydro-elastic system indicated in Fig. 1(a). It is evident that, replacing the impermeability (12) condition with the free surface condition in (13) we obtain the dispersion equation for the hydro-elastic system indicated in Fig. 1(b) which was already considered in the paper by Bagno (2015).

4. Numerical results and discussions

Numerical results which will be considered below are obtained through the numerical solution to the dispersion Eq. (28) under the solution made by employing the well-known “bi-section” method. Before the consideration and analyses of these results we attempt to test the used algorithm for the case where the elastic plate is in contact with the compressible inviscid fluid filled the half-space. Recall that this case was also considered in the paper by Bagno (2017) and instead of the impermeability condition (12) (or instead of the free surface condition (13)) it was assumed the condition $|\varphi| < M = \text{const}$ as $x_2 \rightarrow -\infty$ for the “plate + half-space fluid” (for which $-\infty < x_2 < -h$) system and the constant B_2 in (23) and (25) is taken as zero, i.e., $B_2 = 0$. Here $B_2 = 0$ means that there are no waves reflected from infinity, and $|\varphi| < M = \text{const}$ as $x_2 \rightarrow -\infty$ means that, according to (23) and (24), in the cases where $c > a_0$ (in the case where $c < a_0$) the fluid velocities at “infinity” do not vanish and remain bounded (the fluid flow velocities vanish). Moreover, as in the paper by Bagno (2017) we assume that the material of the elastic layer is glass with the parameters: $\rho = 1160 \text{ kg/m}^3$, $\lambda = 3.96 \times 10^9 \text{ Pa}$, $\mu = 1.86 \times 10^9 \text{ Pa}$ and material of the fluid is water with the parameters: $\rho_0^{(1)} = 1000 \text{ kg/m}^3$ and $a_0 = 1460 \text{ ms}$. Dispersion curves related to this case are given in Fig. 2(a) and in this figure through dashed lines are drawn the dispersion curves related to the Lamb waves obtained for the elastic plate without contacting with the fluid, however, with solid lines are shown the corresponding dispersion curves for the case where the plate is in contact with the fluid half-space, i.e., the dispersion curves related to the quasi-Lamb waves. Moreover, in this figure through A_1 and A_2 (S_1 and S_2) are indicated the dispersion curves related to the first and second asymmetric (symmetric) modes of the Lamb and corresponding quasi-Lamb waves. We recall that under obtaining the dispersion curves related to the asymmetric A_1 and A_2 (to the symmetric S_1 and S_2) modes of the Lamb waves in the plate without contact with the fluid it is assumed that the $u_1(x_1, x_2) = -u_1(x_1, -(x_2 + h))$ and $u_2(x_1, x_2) = u_2(x_1, -(x_2 + h))$ ($u_1(x_1, x_2) = u_1(x_1, -(x_2 + h))$ and $u_2(x_1, x_2) = -u_2(x_1, -(x_2 + h))$). However, under considering the quasi-Lamb waves (i.e., the case where the plate in contact with fluid) these conditions are not acceptable and the dispersion curves for this case are obtained from the solution of the dispersion Eq. (28). Note that the dispersion curves illustrated in Fig. 2 completely

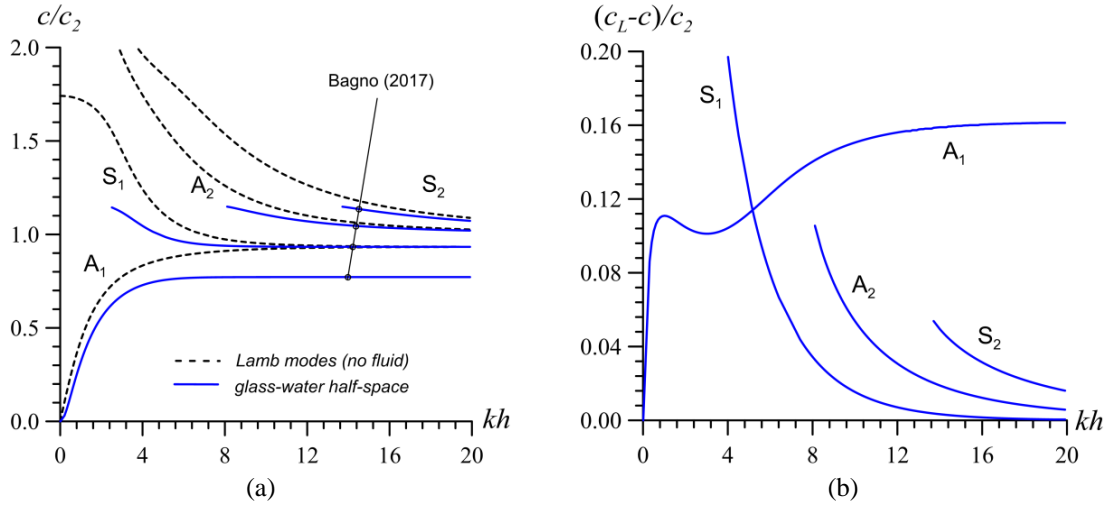


Fig. 2 Dispersion curves for the glass-water half-space vs Lamb waves (no fluid) (a) and the difference between the velocities of the Lamb and quasi-Lamb waves (b)

coincide with the corresponding ones obtained in the paper by Bagno (2017). Moreover, in Fig. 2(b) as an addition to the noted results, the graphs illustrate the difference between the wave propagation velocities obtained for the Lamb and quasi-Lamb waves.

It follows from Fig. 2 that the contact of the plate with the fluid decreases the wave propagation velocity and the cut off wavelength in the first symmetric mode appears. Moreover, it follows from Fig. 2 that the cut off wavelength appear also in the second symmetric and asymmetric modes as a result of the contact of the plate with the fluid. According to Fig. 2, we can conclude that for the selected fluid and plate materials the high wavenumber limit value of the wave propagation velocity in the first asymmetric mode is the corresponding Scholte wave propagation velocity c_{Sch} which is equal to $c_{Sch} = c_{2Gs} \times 0.077171$ for the selected pair of materials (where c_{2Gs} is the shear wave propagation velocity in the selected glass). However, such limit value for the first symmetric mode is the Rayleigh wave propagation velocity c_R in the plate material which is equal to $c_R = c_{2Gs} \times 0.9355$. At the same time, the relation $a_0/c_{2Gs} = 1.1525$ occurs in the case under consideration.

Now we analyze the numerical results obtained for the hydro-elastic system, the sketch of which is illustrated in Fig. 1(a), consisting of the elastic plate, compressible inviscid fluid, and rigid wall. These results are given in Fig. 3 and in this figure for clarity the graphs related to the dispersion curves of the selected modes are given separately. Note that the results given in Fig. 3 are obtained for various values of the ratio h_d/h and from these results we can conclude how the fluid depth can affect the dispersion of the considered waves under the restriction of the flow of this fluid through the rigid wall.

Thus, it follows from the dispersion curves related to the A_1 mode that a decrease in the fluid layer thickness causes the wave propagation velocity to decrease monotonically. Note that this dependence of the wave propagation velocity on the fluid depth agrees with the well-known physicomechanical consideration. However, the analyses of the dispersion curves related to the S_1 mode shows that the character of the influence of the fluid layer thickness on the wave propagation velocity of this mode depends on the values of the dimensionless wavenumber kh , i.e., there exist such value of the kh (denote it by $(kh)_{S_1}$) before which, i.e., under $kh < (kh)_{S_1}$ (after which, i.e., under

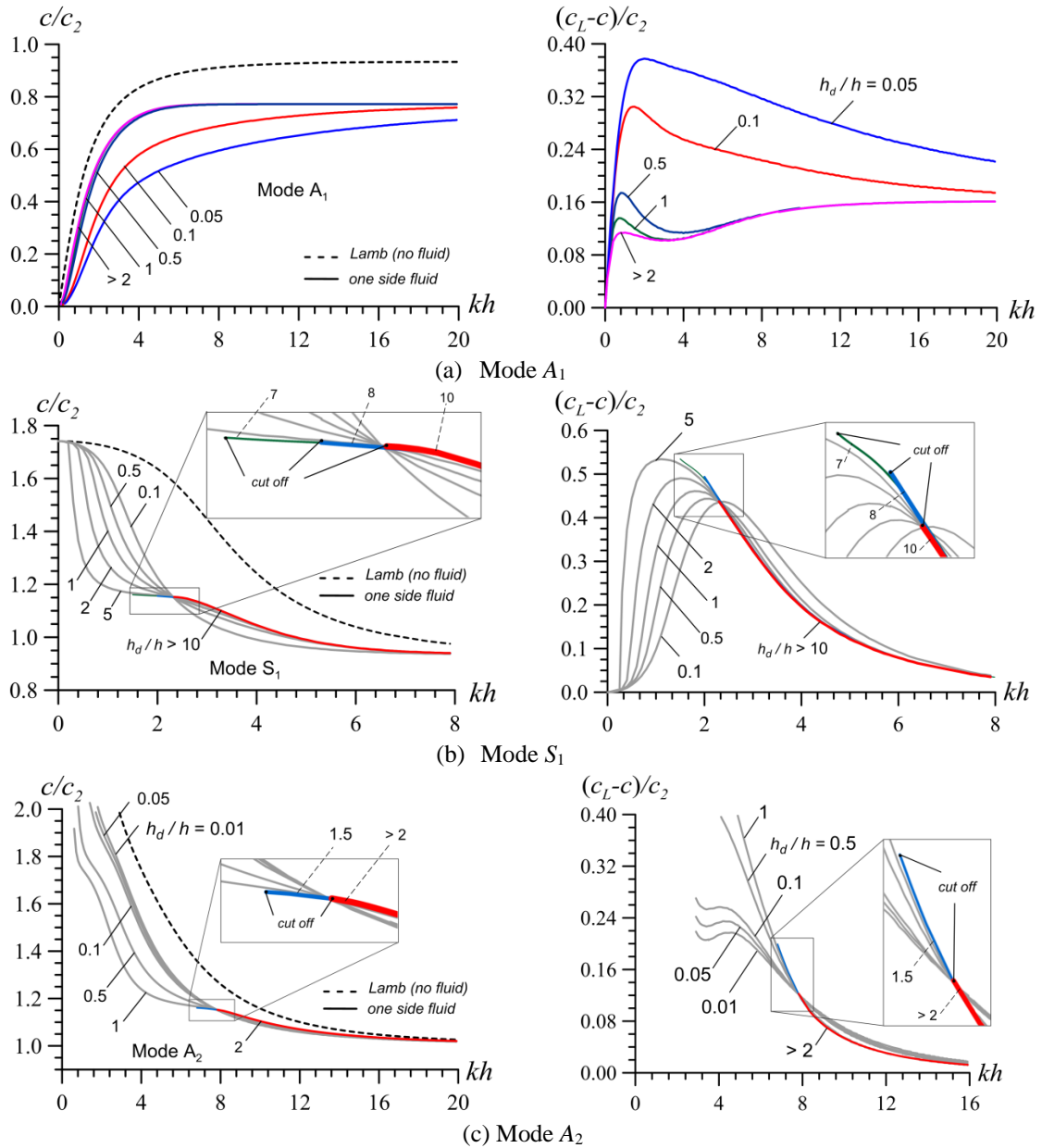


Fig. 3 The dispersion curves of modes A_1 (a), S_1 (b), A_2 (c), and S_2 (d) for the glass-water system for different thicknesses of the fluid layer

$kh > (kh)_{S_1}$) increase in the fluid layer thickness causes the values of the mentioned wave propagation velocity to decrease (to increase). However, where $kh < (kh)_{S_1}$, the magnitude of the effect of fluid layer thickness variation on the wave propagation velocity is more important than in the case where $kh > (kh)_{S_1}$. At the same time, these graphs show that an increase in the thickness of the fluid layer causes to appear the cut-off wavelength with the corresponding cut-off frequency to appear. Note

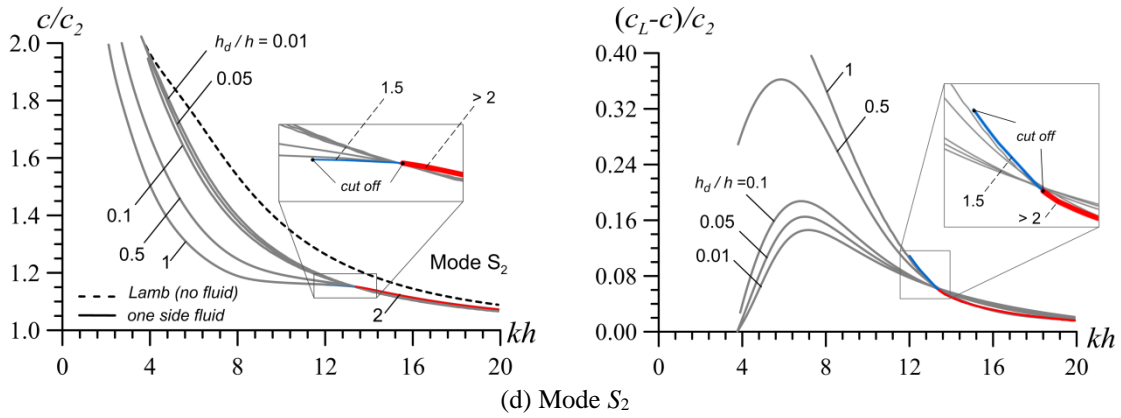


Fig. 3 Continued

that this appearance is observed more clearly in the case where $h_d/h \geq 7$ and the values of the cut-off wavelength increase monotonically with h_d/h .

The analyses of the dispersion curves related to the mode A_2 are similar in the qualitative sense with those obtained for the S_2 mode and as in the mode S_1 there exist such values of the dimensionless wavenumber kh (denote they for the A_2 and S_2 by $(kh)_{S_2}$ and $(kh)_{A_2}$, respectively) before which, i.e., under $kh < (kh)_{A_2}$ and $kh < (kh)_{S_2}$ (after which, i.e., under $kh > (kh)_{A_2}$ and $kh > (kh)_{S_2}$) an increase in the values of the h_d/h causes to decrease (to increase) the wave propagation velocity of the A_2 and S_2 modes. At the same time, it should be noted that the magnitude of the influence of the h_d/h on the wave propagation velocity of the A_2 and S_2 modes in the cases where $kh < (kh)_{A_2}$ and $kh < (kh)_{S_2}$ is more significant than that in the cases where $kh > (kh)_{A_2}$ and $kh > (kh)_{S_2}$. Moreover, the observation of the graphs related to the A_2 and S_2 shows that an increase in the values of the h_d/h causes the cut off wavelength to appear and it follows from these graphs that $(kh)_{S_1} > (kh)_{A_2} > (kh)_{S_2}$.

The detail analyses of the foregoing numerical results show that in the cases where $kh = (kh)_{S_1}$, $kh = (kh)_{A_2}$ and $kh = (kh)_{S_2}$ the wave propagation velocity on the dispersion curves related to the S_1 , A_2 and S_2 modes, respectively, is equal to $c/c_{2G_s} = 1.1525$, i.e., to the $c = a_0$ where a_0 is a sound speed in the water. Namely, in these cases, i.e., in the cases where $kh = (kh)_{S_1}$, $kh = (kh)_{A_2}$ and $kh = (kh)_{S_2}$ the fluid layer thickness does not affect the wave propagation velocity in the hydro-elastic system under consideration and this velocity is equal to the sound speed in the fluid.

Thus, based on this fact and based on the above results we can conclude that the parts of the dispersion curves, where the wave propagation velocity is less than sound speed in the fluid (denote it as the case where $c < a_0$), approach the corresponding ones of the dispersion curves related to the same elastic plate contacting with the same fluid which filled the half-space.

Also, we can conclude that the parts of the dispersion curves, where the wave propagation velocity is greater than sound speed in the fluid (denote it as the case where $c > a_0$) does not approach, i.e., “move away” from the corresponding ones of the dispersion curves related to the same elastic plate contacting with the same fluid which filled the half-space.

Note that these conclusions hold not only for the “glass+water” material pair, as we will consider below, but also for the other plate and fluid material pairs.

Now we consider the case where the material of the plate is steel with parameters $\rho = 7800 \text{ kg/m}^3$,

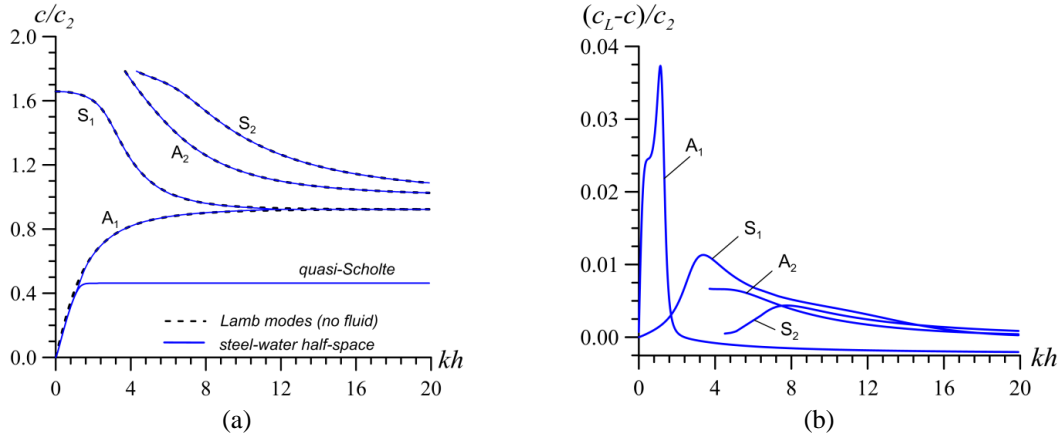


Fig. 4 Dispersion curves for the steel-water half-space vs Lamb waves (no fluid) (a) and difference between wave propagation velocities of the quasi-Lamb and Lamb waves (b)

$\lambda=92.6 \times 10^9$ Pa, $\mu=77.5 \times 10^9$ Pa and the fluid is water with the parameters given above. Dispersion curves for the half-plane fluid case are given in Fig. 4(a) from which we can see that the influence of the fluid existence on the wave propagation velocities in all modes under consideration is insignificant. However, in the steel+water case new wave dispersion mode appear, called the quasi-Scholte mode and wave propagation velocity on this mode tend to the Scholte wave propagation velocity c_{Sch} for the steel+water pair with kh which is equal to $c_{Sch}=c_{2St} \times 0.462886$ where c_{2St} is shear wave propagation velocity in steel. However, the A_1 and S_1 modes wave propagation velocity tend the Rayleigh wave propagation velocity c_R with dimensionless wavenumber kh which is equal to $c_R=c_{2St} \times 0.923008$. At the same time, the relation $a_0/c_{2St}=0.4630$ occurs in the case under consideration. Moreover, in Fig. 4(b) as an addition to the noted results, the graphs illustrate the difference between the wave propagation velocities obtained for the Lamb and quasi-Lamb waves.

Now we consider the dispersion curves obtained for the hydro-elastic system consisting of the elastic plate, of the fluid layer and of the rigid wall which bounded this layer, and study the influence of the ratio h_d/h on the behavior of these curves obtained for the zeroth and the first fourth modes. It should be noted that these modes will be distinguished from each other by the magnitude of the obtained roots from the dispersion Eq. (28) for each selected dimensionless wavenumber kh . The curves constructed by the first root named as the dispersion curve related to the zeroth (or quasi-Scholte wave) mode in the hydro-elastic system under consideration. The dispersion curves obtained for various values of the ratio h_d/h are given in Fig. 5. However, the dispersion curves constructed by the second, third, fourth and fifth roots named as the dispersion curves related to the first, second, third and fourth modes and the dispersion curves related to these modes which are also obtained for various values of the ratio h_d/h are given in Fig. 6. In other words, we will not use names as the A_1 , S_1 , A_2 and S_2 modes in the present case which were used in the previous, i.e., in the “glass+water” case. This is because in the “steel+water” case under moderate values of the ratio h_d/h the aforementioned first, second, third, and fourth modes become significantly differ from the A_1 , S_1 , A_2 and S_2 modes obtained for the plate contacting with the fluid which filled half-space, not only in the quantitative sense but also in the quantitative sense.

Note that the graphs in Fig. 5(b) show the difference between the wave propagation velocities of the Scholte waves obtained for the “plate+fluid+rigid wall” and “plate+half-space fluid” systems.

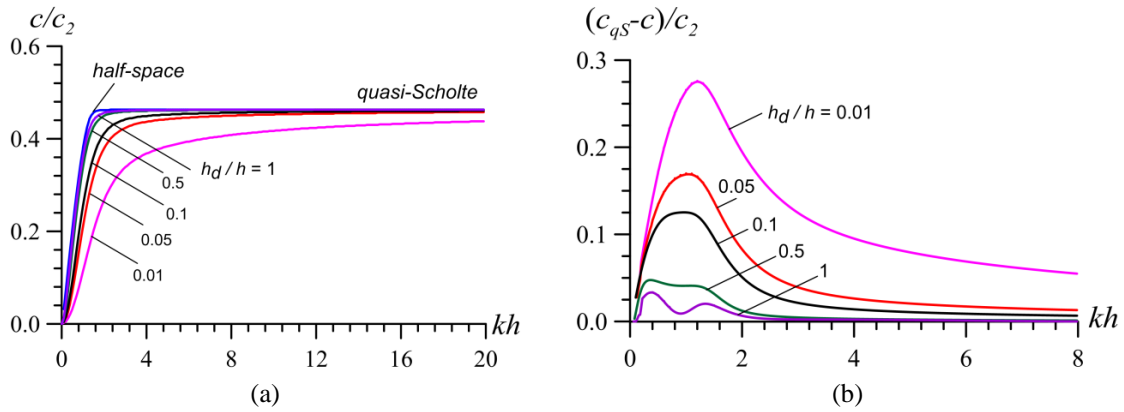


Fig. 5 The dispersion curves of quasi-Scholte mode (zeroth mode) (a) for the steel-water system for different thicknesses of the fluid layer and difference between the wave propagation velocities of the Scholte waves obtained for the “plate+fluid+rigid wall” and “plate+half-space fluid” systems (b)

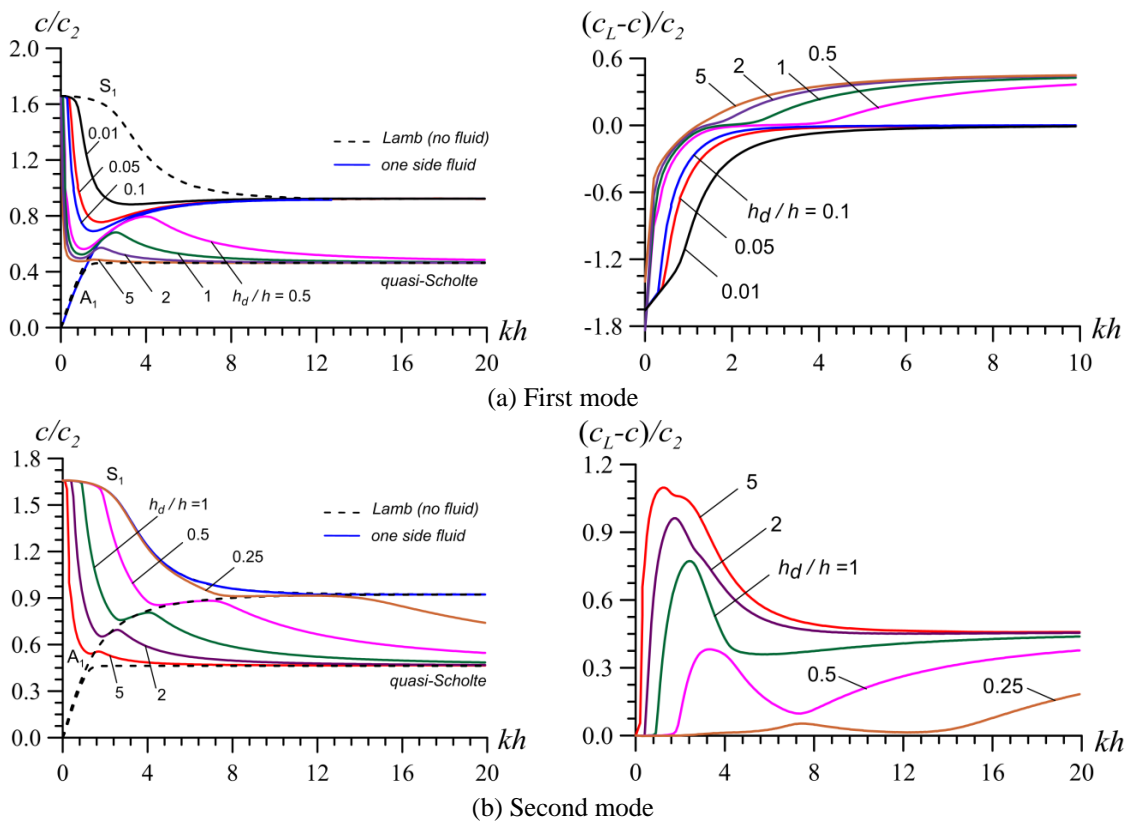
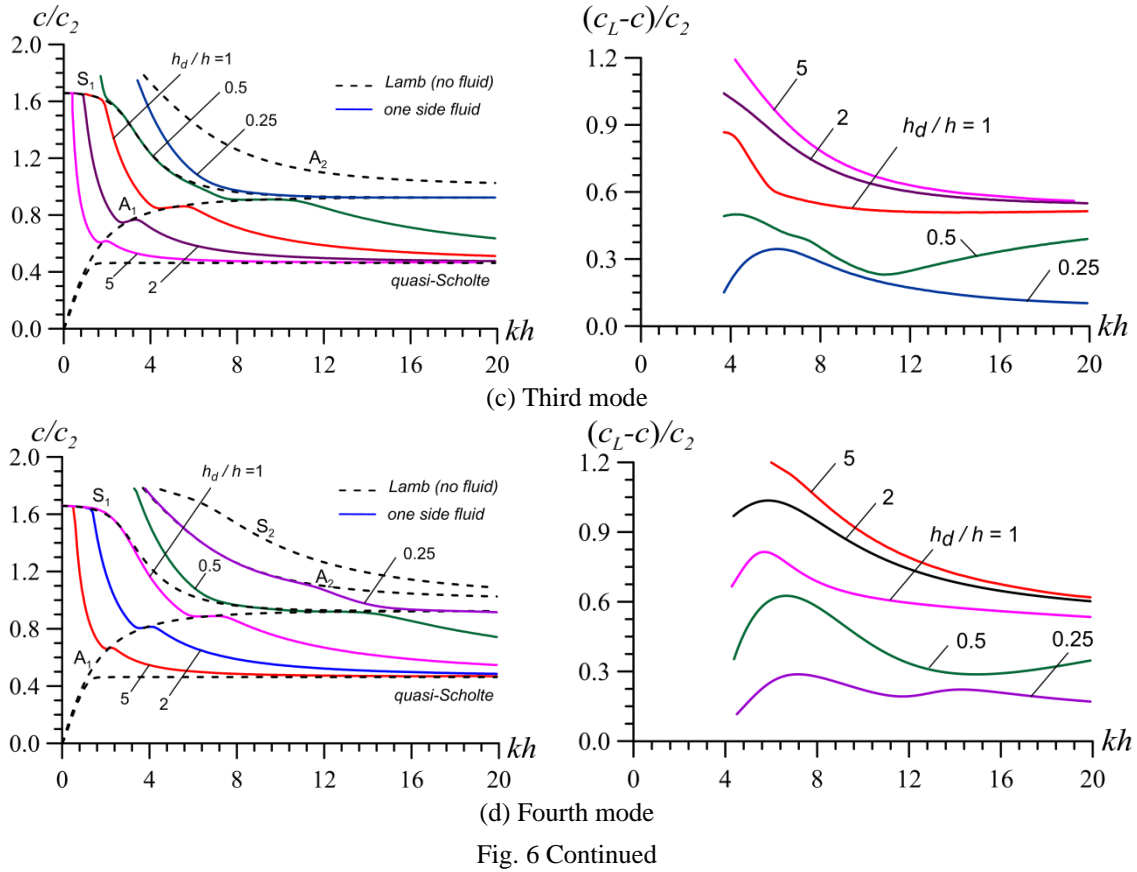


Fig. 6 The dispersion curves of the first (a), second (b), third (c) and fourth (d) modes for the steel-water system for different thicknesses of the fluid layer

Moreover, note that graphs on the right in Fig. 6 show the difference of the wave propagation velocities in the first, second, third and fourth modes obtained for the “plate+fluid+rigid wall”



system from the wave propagation velocities on the dispersion curves of the A_1 , S_1 , A_2 and S_2 modes, respectively, obtained for the “plate+half-space fluid” system.

Thus, according to relation $a_0/c_{2S_1}=0.4630$ for the “steel+water” pair and according to the conclusion made above on the character of the influence of h_d/h on the dispersion curves constructed for the hydro-elastic system under consideration, the parts of the dispersion curves or the whole dispersion curves on which the wave propagation velocity c is less than a_0 a decrease in the values of the ratio h_d/h must decrease the wave propagation velocity with respect to the corresponding velocities obtained for the “plate+half-space fluid” system. However, an increase in the values of the ratio h_d/h must approach the wave propagation velocity obtained for the system under consideration to the corresponding velocities obtained for the “plate+half-space fluid” system. The analyses of the graphs given in Fig. 5 confirm this prediction.

For all the selected values of the ratio h_d/h , the dispersion curves related to the first mode starts from the near vicinity of the low-wavenumber limit value of the wave propagation velocity related to the mode A_1 obtained for the “plate+half-space fluid system”. In the relatively small values of the ratio h_d/h (for instance, in the cases where $h_d/h \leq 0.1$) the wave propagation velocity in this mode tends to the Rayleigh wave propagation velocity for the plate material with the dimensionless wavenumber kh . However, for the relatively great values of the ratio h_d/h (for instance in the cases where $h_d/h \geq 0.5$) these velocities tend to the Scholte wave propagation velocity for the “steel+water”

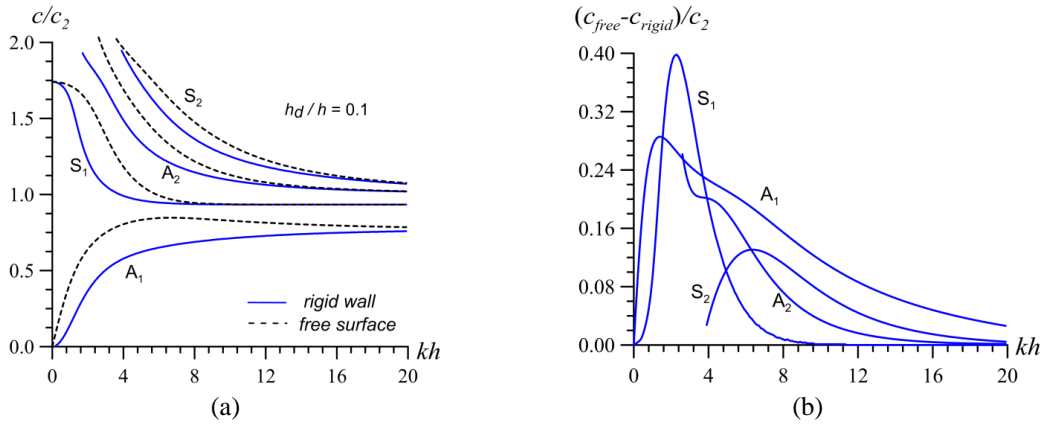


Fig. 7 Dispersion curves for the glass-water case for the “plate+fluid layer+rigid wall” (a) and for the “plate+fluid layer+free face” (b) systems

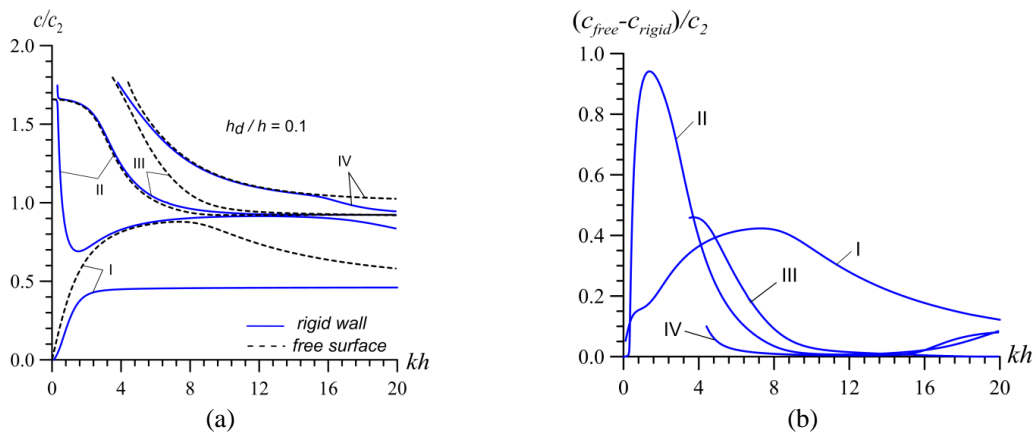


Fig. 8 Dispersion curves for the steel-water case for the “plate+fluid layer+rigid wall” (a) and for the “plate+fluid layer+free face” (b) systems

system with the dimensionless wavenumber kh . At the same time, in the relatively small values of the ratio h_d/h (i.e., in the cases where $h_d/h \leq 0.1$) after a certain value of the kh , the dispersion curves of the first mode merge with the dispersion curve related to the mode A_1 obtained for the “plate+half-space fluid case”. However, in the relatively great values of the ratio h_d/h (i.e., in the cases where $h_d/h \geq 0.5$) after a certain value of the kh , the dispersion curves related to the first mode have contact parts with dispersion curve of the aforementioned A_1 mode and after this contact part, these curves tend, as noted above, to the Scholte wave propagation velocity obtained for the “steel+water” system with the dimensionless wavenumber kh . It follows from the foregoing results that the wave propagation velocities of all the dispersion curves related to the first mode are greater than the sound speed in the water, i.e., the case where $c > a_0$ takes place. Moreover, it follows from these results that for the relatively small values of the ratio h_d/h (i.e., in the cases where $h_d/h \leq 0.1$) the dispersion curves obtained for the first mode after a certain value of the kh become very close to the dispersion curve obtained for the mode A_1 , however, in the relatively great values of the ratio h_d/h (i.e., in the cases where $h_d/h \geq 0.5$) the dispersion curves related to the first mode “move away” from the dispersion

curve related to the mode A_1 with h_d/h . Consequently, the results obtained for the first mode is also agree with the conclusion made above on the character of the influence of the h_d/h on the dispersion curves. This conclusion is also confirmed by the dispersion curves obtained for the dispersion curves related to the second mode. To be more precise, for the relatively small values of the ration h_d/h (for instance in the cases where $h_d/h \leq 0.1$) the dispersion curves obtained for the second mode becomes very close to the dispersion curve obtained for the S_1 mode obtained for the “plate+half-space fluid” system and in these cases, the wave propagation velocity on these dispersion curves tend to the Rayleigh wave propagation velocity of the steel with the wavenumber kh . However, under the relatively great values of the ratio h_d/h (for instance in the cases where $h_d/h \geq 0.5$) the dispersion curves obtained for the second mode “move away” from the dispersion curve related to the mode S_1 with the h_d/h and the wave propagation velocity on these curves tend to the Scholte wave propagation velocity for the “steel+water” pair.

Almost the same situation, i.e., the situation observed for the dispersion curves related to the second mode, takes place also for the dispersion curves related to the third and fourth modes. However, the dispersion curves related to the third and fourth modes must be compared with the S_2 and A_2 modes, respectively, regarding the “plate+half-space fluid system.

Finally, we consider the comparison of the dispersion curves obtained within the scope of the impermeability condition (12) (Fig. 1(a)) with corresponding ones obtained within the scope of the free face condition (13) (Fig. 1(b)). For this purpose, we consider the graphs presented in Figs. 7 and 8 which illustrate the dispersion curves related to the “glass+water” and “steel+water” systems, respectively. It follows from these results that as a result of the impermeability condition the wave propagation velocity decrease with respect to the corresponding ones obtained for the free face condition. Moreover, according to the foregoing conclusions on the behavior of the dispersion curves with respect to the ratio c/a_0 , it can be also concluded that the parts of the dispersion curves obtained for the system “plate+fluid+rigid wall” on which the wave propagation velocity c is less (greater) than sound speed a_0 in the fluid must (must not) approach the corresponding ones obtained for the system “plate+fluid layer with free surface”. These features make it necessary to carry out the investigations presented in this work.

5. Conclusions

Thus, in the present paper, for the first time, it is studied the dispersion of the longitudinal waves propagated in the hydro-elastic system consisting of an elastic plate, compressible inviscid fluid and rigid wall restricted the motion of the plate. The novelty of the investigations consists namely of taking the existence and influence of the rigid wall that restricted the flow of the fluid into consideration on the dispersion on mentioned waves. The motion of the plate is described with exact equations and relations of elastodynamics and the flow of the fluid with the linearized Navier-Stokes equations and corresponding linearized relations for compressible barotropic inviscid fluid. The corresponding dispersion equation is obtained and solved numerically for two pairs of the plate and fluid materials: namely “glass+water” and “steel+water” systems. The obtained numerical results are compared with the corresponding results obtained for the corresponding hydro-elastic systems consisting of the same plate and of the same fluid which is filled the half-space. The main focus in these investigations is how the change of the fluid layer thickness, i.e., the ratio h_d/h (where h_d is the fluid layer thickness or fluid depth, h is the plate thickness) influences the dispersion of the propagating waves under impermeability condition on the rigid wall. The most important conclusion

obtained from these investigations can be formulated as follows:

- Parts of the dispersion curves on which the wave propagation velocity is less than the sound speed in the fluid tend to the corresponding parts of the dispersion curves obtained for the “plate+half-space fluid” system. Moreover, the increase in the ratio h_d/h causes the wave propagation velocity to increase in the mentioned parts of the dispersion curves;
- Parts of the dispersion curves on which the wave propagation velocity is greater than the sound speed in the fluid “move away” from the corresponding parts of the dispersion curves obtained for the “plate+half-space fluid” system and in general, the decrease (the increase) in the ratio h_d/h causes the wave propagation velocity in the mentioned parts of the dispersion curves to increase (to decrease);

Based on the above results, in the text of the paper it is made more concrete conclusions on the influence of the problem parameters on the wave dispersion propagating in the considered hydro-elastic systems.

References

- Akbarov, S.D. (2018), “Forced vibration of the hydro-viscoelastic and-elastic systems consisting of the viscoelastic or elastic plate, compressible viscous fluid and rigid wall: A review”, *Appl. Math. Comput.*, **17**(3), 221-245.
- Akbarov, S.D. and Huseynova, T.V. (2019), “Forced vibration of the hydro-elastic system consisting of the orthotropic plate, compressible viscous fluid and rigid wall”, *Coupl. Syst. Mech.*, **8**(3), 199-218. <http://doi.org/10.12989/csm.2019.8.3.199>.
- Akbarov, S.D. and Huseynova, T.V. (2020), “Fluid flow profile in the “orthotropic plate+compressible viscous fluid+rigid wall” system under the action of the moving load on the plate”, *Coupl. Syst. Mech.*, **9**(3), 289-309. <http://doi.org/10.12989/csm.2020.9.3.289>.
- Akbarov, S.D. and Ismailov, M.I. (2015), “Dynamics of the moving load acting on the hydro-elastic system consisting of the elastic plate, compressible viscous fluid and rigid wall”, *Comput. Mater. Contin.*, **45**(2), 75-105.
- Akbarov, S.D. and Ismailov, M.I. (2016), “Dynamics of the oscillating moving load acting on the hydroelastic system consisting of the elastic plate, compressible viscous fluid and rigid wall”, *Struct. Eng. Mech.*, **59**(3), 403-430. <http://doi.org/10.12989/sem.2016.59.3.403>.
- Akbarov, S.D. and Ismailov, M.I. (2017), “The forced vibration of the system consisting of an elastic plate, compressible viscous fluid and rigid wall”, *J. Vib Control*, **23**(11), 1809-1827. <https://doi.org/10.1177/1077546315601299>.
- Akbarov, S.D. and Ismailov, M.I. (2018), “The influence of the rheological parameters of a hydro-viscoelastic system consisting of a viscoelastic plate, viscous fluid and rigid wall on the frequency response of this system”, *J. Vib. Control*, **24**(7), 1341-1363. <https://doi.org/10.1177/1077546316660029>.
- Akbarov, S.D. and Panakhli, P.G. (2017), “On the particularities of the forced vibration of the hydro-elastic system consisting of a moving elastic plate, compressible viscous fluid and rigid wall”, *Coupl. Syst. Mech.*, **6**(3), 287-316. <https://doi.org/10.12989/csm.2017.6.3.287>.
- Bagno, A.M. (1997), “Elastic waves in prestressed bodies interacting with a fluid (Survey)”, *Int. Appl. Mech.*, **33**(6), 435-463. <https://doi.org/10.1007/BF02700652>.
- Bagno, A.M. (2015), “The dispersion spectrum of a wave process in a system consisting of an ideal fluid layer and a compressible elastic layer”, *Int. Appl. Mech.*, **51**(6), 648-653. <https://doi.org/10.1007/s10778-015-0721-7>
- Bagno, A.M. (2016), “Wave propagation in an elastic layer interacting with a viscous liquid layer”, *Int. Appl. Mech.*, **52**(2), 133-139. <https://doi.org/10.1007/s10778-016-0740-z>.
- Bagno, A.M. (2017), “Dispersion properties of lamb waves in an elastic layer-ideal liquid half-space system”,

- Int. Appl. Mech.*, **53**(6), 609-616. <https://doi.org/10.1007/s10778-018-0843-9>.
- Bagno, A.M. and Guz, A.N. (2016), "Effect of prestresses on the dispersion of waves in a system consisting of a viscous liquid layer and a compressible elastic layer", *Int. Appl. Mech.*, **52**(4), 333-341. <https://doi.org/10.1007/s10778-018-0843-9>.
- Guz, A.N. (2009), *Dynamics of Compressible Viscous Fluid*, Cambridge Scientific Publishers, Cambridge, England.
- Guz, A.N. and Bagno, A.M. (2019), "Propagation of quasi-lamb waves in an elastic layer interacting with a viscous liquid half-space", *Int. Appl. Mech.*, **55**(5), 459-469. <https://doi.org/10.1007/s10778-019-00968-w>.
- Moreno-Navarro, P., Ibrahimbegovic, A. and Ospina, A. (2020), "Multi-field variational formulations and mixed finite element approximations for electrostatics and magnetostatics", *Comput. Mech.*, **65**(1), 41-59. <https://doi.org/10.1007/s00466-019-01751-x>.
- Moreno-Navarro, P., Ibrahimbegovic, A. and Perez-Aparicio, J.L. (2018), "Linear elastic mechanical system interacting with coupled thermo-electro-magnetic fields", *Coupl. Syst. Mech.*, **7**, 5-25. <https://doi.org/10.12989/csm.2018.7.1.005>.
- Moreno-Navarro, P., Ibrahimbegovic, A. and Perez-Aparicio, J.L. (2017), "Plasticity coupled with thermo-electric fields: Thermodynamics framework and finite element method computations", *Comput. Meth. Appl. Mech. Eng.*, **315**, 50-72. <https://doi.org/10.1016/j.cma.2016.10.038>.
- Viktrov, I.A. (1967), *Rayleigh and Lamb Waves, Physical Theory and Applications*, Acoustics Institute, Academy of Science of the USSR, Moscow, Russia.

Appendix

We attempt to explain how the linearized equations in (4) and (5) are obtained from the corresponding non-linear equations and for this purpose we write the corresponding non-linear equations.

The non-linear Navier-Stokes equations for inviscid fluid

$$\rho \left(\frac{\partial V_1}{\partial t} + V_1 \frac{\partial V_1}{\partial x_1} + V_2 \frac{\partial V_1}{\partial x_2} \right) + \frac{\partial p}{\partial x_1} = 0, \quad \rho \left(\frac{\partial V_2}{\partial t} + V_1 \frac{\partial V_2}{\partial x_1} + V_2 \frac{\partial V_2}{\partial x_2} \right) + \frac{\partial p}{\partial x_2} = 0. \quad (\text{A1})$$

The continuity equation

$$\frac{\partial \rho}{\partial t} + \frac{\partial}{\partial x_1}(\rho V_1) + \frac{\partial}{\partial x_2}(\rho V_2) = 0. \quad (\text{A2})$$

We represent the velocities V_1 and V_2 , density ρ and pressure p as a summation of the initial and perturbed states, i.e., as follows

$$V_1 = V_1^{(0)} + v_1, \quad V_2 = V_2^{(0)} + v_2, \quad \rho = \rho^{(0)} + \rho^{(1)}, \quad p = p^{(0)} + p^{(1)}, \quad (\text{A3})$$

where $V_1^{(0)}$ and $V_2^{(0)}$ are velocities, $\rho^{(0)}$ is density and $p^{(0)}$ is pressure of the fluid in the initial state, $v_1, v_2, \rho^{(1)}$ and $p^{(1)}$ are perturbations of the corresponding quantities.

We rewrite equations in (A1) and (A2) taking the expressions in (A3) into account.

$$\begin{aligned} & (\rho^{(0)} + \rho^{(1)}) \left(\frac{\partial (V_1^{(0)} + v_1)}{\partial t} + (V_1^{(0)} + v_1) \frac{\partial (V_1^{(0)} + v_1)}{\partial x_1} + (V_2^{(0)} + v_2) \frac{\partial (V_1^{(0)} + v_1)}{\partial x_2} \right) + \frac{\partial (p^{(0)} + p^{(1)})}{\partial x_1} = 0, \\ & (\rho^{(0)} + \rho^{(1)}) \left(\frac{\partial (V_2^{(0)} + v_2)}{\partial t} + (V_1^{(0)} + v_1) \frac{\partial (V_2^{(0)} + v_2)}{\partial x_1} + (V_2^{(0)} + v_2) \frac{\partial (V_2^{(0)} + v_2)}{\partial x_2} \right) + \frac{\partial (p^{(0)} + p^{(1)})}{\partial x_2} = 0. \end{aligned} \quad (\text{A4})$$

$$\frac{\partial (\rho^{(0)} + \rho^{(1)})}{\partial t} + \frac{\partial}{\partial x_1}((\rho^{(0)} + \rho^{(1)})(V_1^{(0)} + v_1)) + \frac{\partial}{\partial x_2}((\rho^{(0)} + \rho^{(1)})(V_2^{(0)} + v_2)) = 0. \quad (\text{A5})$$

As in the case under consideration it is assumed that $V_1^{(0)} = V_2^{(0)} = 0$, $\rho^{(0)} = \text{const}$ and $p^{(0)} = \text{const}$, therefore we obtain the following expressions for the equations in (A4) and (A5).

$$(\rho^{(0)} + \rho^{(1)}) \left(\frac{\partial v_1}{\partial t} + v_1 \frac{\partial v_1}{\partial x_1} + v_2 \frac{\partial v_1}{\partial x_2} \right) + \frac{\partial p^{(1)}}{\partial x_1} = 0, \quad (\rho^{(0)} + \rho^{(1)}) \left(\frac{\partial v_2}{\partial t} + v_1 \frac{\partial v_2}{\partial x_1} + v_2 \frac{\partial v_2}{\partial x_2} \right) + \frac{\partial p^{(1)}}{\partial x_2} = 0. \quad (\text{A6})$$

$$\frac{\partial \rho^{(1)}}{\partial t} + \frac{\partial}{\partial x_1}((\rho^{(0)} + \rho^{(1)})v_1) + \frac{\partial}{\partial x_2}((\rho^{(0)} + \rho^{(1)})v_2) = 0. \quad (\text{A7})$$

We represent the equations in (A6) and (A7) in the following form.

$$\rho^{(0)} \frac{\partial v_1}{\partial t} + \frac{\partial p^{(1)}}{\partial x_1} + \rho^{(1)} \left(\frac{\partial v_1}{\partial t} + v_1 \frac{\partial v_1}{\partial x_1} + v_2 \frac{\partial v_1}{\partial x_2} \right) + \rho^{(0)} \left(v_1 \frac{\partial v_1}{\partial x_1} + v_2 \frac{\partial v_1}{\partial x_2} \right) = 0,$$

$$\rho^{(0)} \frac{\partial v_2}{\partial t} + \frac{\partial p^{(1)}}{\partial x_2} + \rho^{(1)} \left(\frac{\partial v_2}{\partial t} + v_1 \frac{\partial v_2}{\partial x_1} + v_2 \frac{\partial v_2}{\partial x_2} \right) + \rho^{(0)} \left(v_1 \frac{\partial v_2}{\partial x_1} + v_2 \frac{\partial v_2}{\partial x_2} \right) = 0. \quad (\text{A8})$$

$$\frac{\partial \rho^{(1)}}{\partial t} + \rho^{(0)} \left(\frac{\partial v_1}{\partial x_1} + \frac{\partial v_2}{\partial x_2} \right) + \frac{\partial}{\partial x_1} (\rho^{(1)} v_1) + \frac{\partial}{\partial x_2} (\rho^{(1)} v_2) = 0. \quad (\text{A9})$$

Assuming that the quantities of the perturbations v_1 , v_2 , $\rho^{(1)}$ and $p^{(1)}$ are so small that the underlined non-linear terms in Eqs. (A8) and (A9) can be neglected with respect to the no-underlined linear terms and this neglecting is called the linearization, as a result of which it is obtained the following linearized Navier-Stokes equations for inviscid fluid

$$\rho^{(0)} \frac{\partial v_1}{\partial t} + \frac{\partial p^{(1)}}{\partial x_1} = 0, \quad \rho^{(0)} \frac{\partial v_2}{\partial t} + \frac{\partial p^{(1)}}{\partial x_2} = 0, \quad (\text{A10})$$

and linearized continuity equation

$$\frac{\partial \rho^{(1)}}{\partial t} + \rho^{(0)} \left(\frac{\partial v_1}{\partial x_1} + \frac{\partial v_2}{\partial x_2} \right) = 0. \quad (\text{A11})$$

Note that the equation in (A10) coincide with the equations in (4), and Eq. (A11) coincides with Eq. (5).